
ORGANIC SYNTHESIS
AND INDUSTRIAL ORGANIC CHEMISTRY

Synthesis of Reduced Graphene Oxide and Its Electrocatalytic Properties

M. O. Danilov, I. A. Slobodyanyuk, I. A. Rusetskii, and G. Ya. Kolbasov

Institute of General and Inorganic Chemistry, National Academy of Sciences of Ukraine, Kiev, Ukraine

Received April 5, 2013

Abstract—The method of the chemical synthesis of reduced graphene oxide was developed. Sodium hypophosphite and sulfite were used as reducing agents. The formation of reduced graphene oxide was confirmed by several methods. Volt-ampere characteristics of electrodes based on reduced graphene oxide were investigated in an experimental model of an oxygen fuel cell with an alkaline electrolyte. Characteristics of oxygen electrodes based on reduced graphene oxide were stable over semiannual tests. The resulting reduced graphene oxide is a promising material for oxygen electrodes of chemical current sources.

DOI: 10.1134/S107042721306013X

Application of air or oxygen electrodes in devices generating electrical energy is rather promising, as it does not trouble ecology and makes it possible to save natural resources such as petroleum and gas. Air and oxygen electrodes in current sources represent a three-phase system electrode–electrolyte–gas, where processes of electric current generation are localized at the boundary between these phases. The current generated on such a gas-diffusion electrode depends on the size of the triple contact zone between these three phases. The electrode consists of a catalyst and a carrier, and the interaction between them basically defines the value of generated current strength. At present the most effective catalyst of oxygen reduction is platinum, however it has an essential drawback, a high price. There are a great number of works dedicated to the study of other effective catalysts [1]. Another important problem concerns a catalytically active and stable catalyst carrier. The advantage of carbon nanotubes as carrying agents of catalysts has been shown in the publications [2–5].

At present owing to the appearance of the new nano-carbon material graphene a series of works were dedicated to its studying as an electrode material for lithium-ionic accumulators [6] and also as a catalyst carrier in fuel cells [7–11]. Graphene is a carbon layer of one atom thickness consisting of condensed six-membered rings.

Carbon atoms in graphene are bound by sp^2 bonds into a hexagonal two-dimensional (2D) lattice. Ideal graphene consists exclusively of six-membered rings; appearance of defects results in the formation of a quantity of five- or seven-membered rings in the graphene structure and hence in the bending of a flat surface. At the same time the extended π -system of conjugated aromatic rings makes graphene rather stable as compared with others nanosubjects. Structural features of graphene sheets are those that charge carriers, having unlimited freedom of transition in the plane, are closed in the narrow space between “walls” arranged at the shortest atomic distance from each other of ~ 0.3 nm, which results in the appearance of graphene unique electrophysical characteristics and other unusual properties (Fig. 1).

In this connection it is of a great interest to study electrochemical properties of reduced graphene oxide (RGO) used as a catalyst carrier for fuel cell oxygen electrodes in relation to the method of its production.

EXPERIMENTAL

Multiwall carbon nanotubes (MCNT) were selected as precursors, because their structure reminds a set of graphene layers coiled into a tube. Using a strong oxidizing agent, it is possible “to unzip” nanotube with the

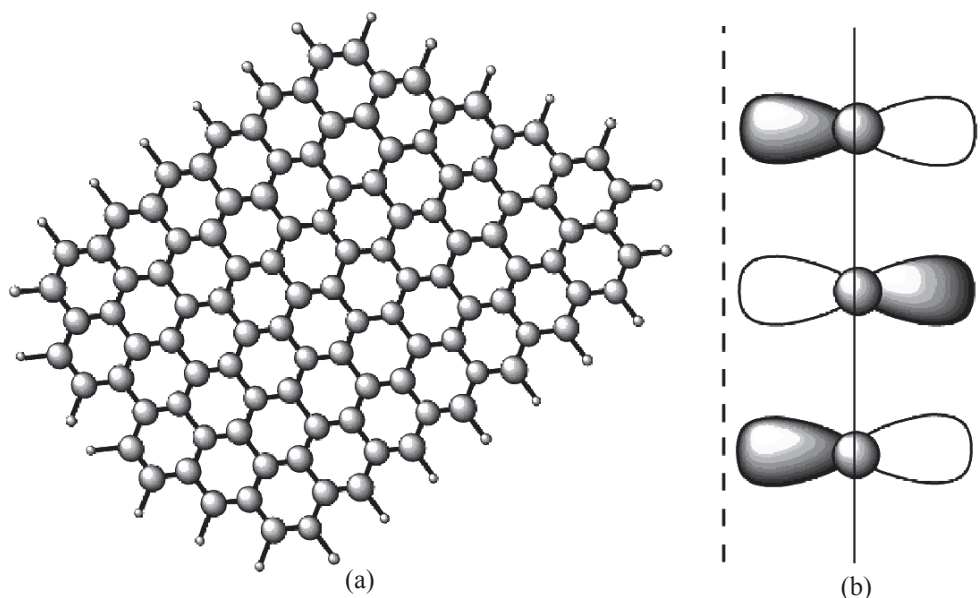


Fig. 1. Schematic structure of graphene. (a) dorsal view, (b) lateral view.

formation of nanotapes of oxidized graphene [12]. For this purpose we have chosen the procedure of the MCNT oxidation by septivalent manganese [12] with postreduction. We used alkaline solutions of sodium hypophosphite and sulfite as reducing agents for oxidized graphene.

Double-layer oxygen electrodes were prepared by pressing. The hydrophobic layer contained 0.07 g cm^{-2} of acetylene black with 25% of polytetrafluoroethylene, the active layer contained 0.02 g cm^{-2} RGO with 5% of polytetrafluoroethylene. Experiments were carried out with a fuel cell model using a zinc electrode as the anode. The experimental model for testing gas-diffusion electrodes is described in the work [13]. A solution of 5 M KOH with 1 M LiOH served as an electrolyte. A silver chloride electrode connected through a salt bridge was used as a reference electrode. All potentials were measured and given with respect to standard silver chloride electrode. Electrochemical load characteristics were obtained in a galvanostatic mode. A U-tube electrolyzer with the alkaline electrolyte was a source of oxygen. Oxygen moved to gas electrodes under excess pressure of 0.01 MPa. Before measurements the oxygen electrode was blown through by oxygen within 1 h. Electronic microphotographs were taken by means of a JEM-100 CXII electronic microscope. The X-ray analysis was carried out on a DRON-4 X-ray diffractometer with $\text{Cu}_{K\alpha}$ radiation. Electronic absorption spectra were recorded on a Perkin Elmer UV/VIS Lambda 35 spectrophotometer.

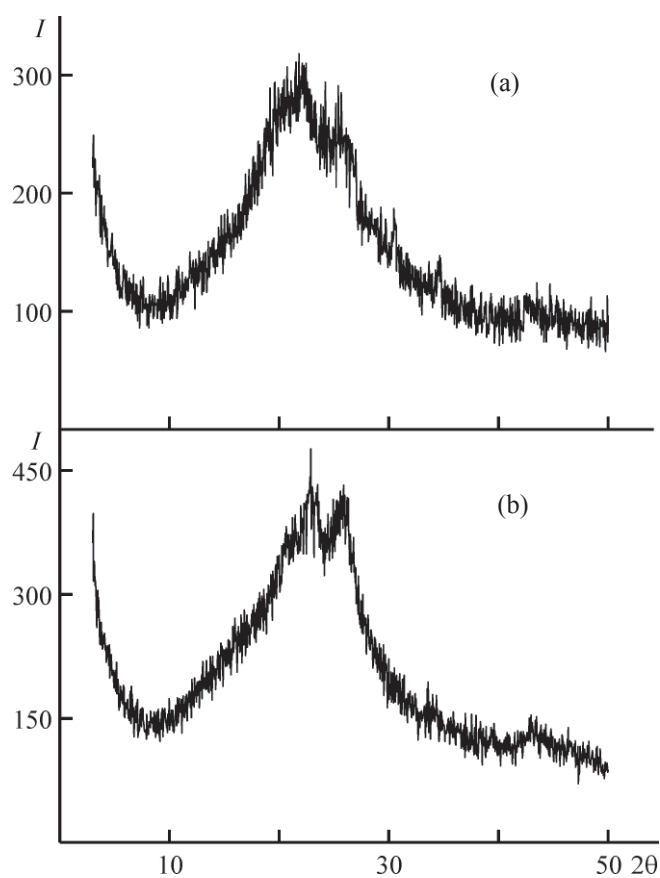


Fig. 2. X-ray pattern of graphene oxide samples reduced by: (a) sodium hypophosphite and (b) sodium sulfite. (I) intensity (arbitrary unit), (2θ) Bragg angle (degree).

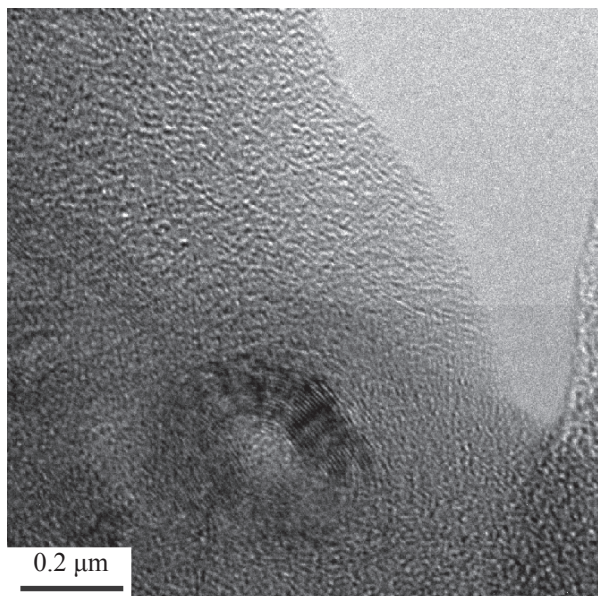


Fig. 3. Microphotograph of a graphene oxide sample reduced by sodium sulfite.

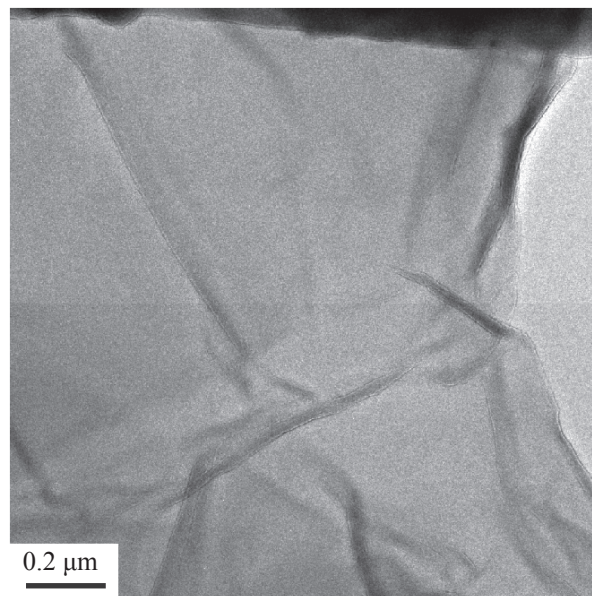


Fig. 4. Microphotograph of a graphene oxide sample reduced by sodium hypophosphite.

To synthesize oxidized graphene, we applied Hummers' modified method [12, 14], using MCNT with bulk weight of $25\text{--}30\text{ g dm}^{-3}$ treated by a hydrofluoric acid solution to remove catalyst admixtures. The external diameter of nanotubes was $10\text{--}30\text{ nm}$ and specific surface area, $230\text{ m}^2\text{ g}^{-1}$.

An MCNT sample of 1 g was dispersed within 1 h by stirring in 300 ml of concentrated sulfuric acid. Then 5 g of KMnO_4 were added with stirring within 1 h at a temperature not higher than 17°C . After that the mixture was heated up to 55°C for 30 min on a water bath and kept for 1 h . Then temperature of the solution was brought to 65°C and it was left to cool down to room temperature. To prevent the formation of manganese dioxide, the resulting mixture was diluted by 400 ml of bidistilled water with ice, which contained 5 ml of $30\text{ H}_2\text{O}_2$. Then the dilute mixture was filtered on a narrow-porous paper filter. The filtered precipitate was dispersed in bidistilled water. Two samples were chosen to be reduced. One sample of the oxidized product was reduced with an alkaline sodium hypophosphite solution ($\text{pH } 11$), another, with an alkaline sodium sulfite solution ($\text{pH } 11$). The reduced substance was filtered on a narrow-porous paper filter, then separated from the filter, and dried up in a drying oven at 140°C within 3 h . The solid filtrate was investigated by electron microscopy and X-ray analysis and the liquid filtrate, by spectral photometry.

Figure 2 contains the X-ray patterns of products obtained by reduction with sodium hypophosphite (curve 1) and sodium sulfite (curve 2). It is seen from the X-ray patterns that RGO is first divided into separate layers and then is agglomerated, the main peak being observed at $2\theta \approx 23\text{--}24^\circ$ [15]. An analysis of the published data allows us to estimate the distance between layers at $3.7\text{--}3.8\text{ \AA}$

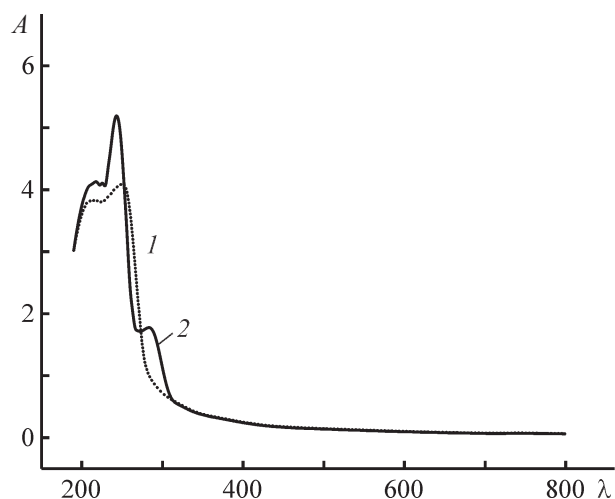


Fig. 5. Absorption spectra of graphene oxide reduced by (1) sodium hypophosphite and (2) sodium sulfite. (*A*) absorption (relative units). Cell thickness 1 cm . (λ) wave length (nm).

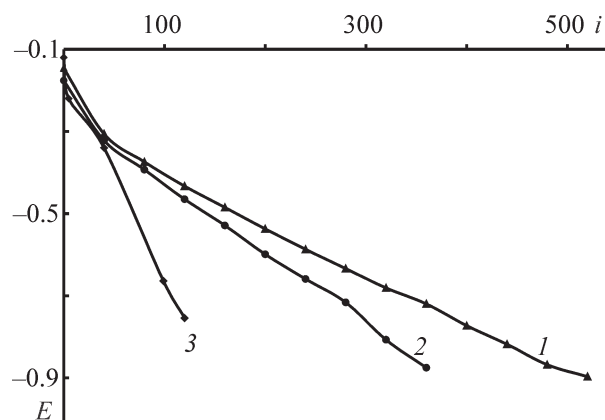


Fig. 6. Volt-ampere characteristics of oxygen electrodes with an active layer of 0.02 g cm^{-2} based on graphene oxide reduced by (1) sodium hypophosphite and (2) sodium sulfite. (E) is potential (V), (i) current density (mA cm^{-2}). (3) initial multiwall carbon nanotubes.

[15–17]. Microphotographs of RGO obtained by the use of various reducing agents are shown in Figs. 3 and 4. The absorption spectrum of an alkaline RGO dispersion (pH 11) in the range of 200–800 nm is shown in Fig. 5. Apparently, the absorption peak of the RGO variance lies within the range of 231–270 nm [18–26]. The main peak at $\sim 250 \text{ nm}$ is connected with the π - π^* -transition of C–C and C=C bonds in the region of the sp^2 -hybridization and the inflection at $\sim 300 \text{ nm}$, with the n - π^* -transition of C=O bonds in the sp^3 -hybridization region [23, 27, 28].

Thus, the study of the absorption spectra of the RGO variance, the analysis of electronic microphotographs, and the comparison of peaks in X-ray patterns with published data allow us to conclude that the described procedure yields nanosheets of reduced graphene oxide.

The obtained oxygen electrodes with active RGO layer were investigated on a model oxygen fuel cell with an alkaline electrolyte. Electrodes with an active layer of initial MCNT were made for comparison.

Volt-ampere characteristics for the obtained oxygen electrodes were measured. Figure 6 presents dependences of the potential on the current density for oxygen electrodes based on graphene oxide reduced by sodium hypophosphite (RGO-GH; curve 1) and by sodium sulfite (RGO-CH; curve 2). For comparison characteristics of electrodes with initial MCNT are given (Fig. 6, curve 3). It is seen from Fig. 6 that the oxygen electrodes based on RGO-GH have the best characteristics.

It has been found that the volt-ampere characteristics

of the oxygen reduction for the RGO-GH electrode 3–4 times exceed those for the initial MCNT electrode. The electrodes based on RGO also surpass those based on the MCNT- MnO_2 nanocomposite, as follows from the comparison with the data of [2]. The characteristics of oxygen electrodes based on reduced graphene oxide were stable over semiannual tests.

CONCLUSIONS

The proposed procedure of graphene oxide reduction makes it possible to obtain high-performance materials for oxygen electrodes of chemical current sources. The procedure of the synthesis is adaptable to streamlined production and does not demand application of high-toxic reagents.

REFERENCES

1. Bidault, F., Brett, D.J.L., Middleton, P.H., and Brandon, N.P., *J. Power Sources*, 2009, vol. 187, no. 1, pp. 39–48.
2. Soehn, M., Lebert, M., Wirth, T., et al., *J. Power Sources*, 2008, vol. 176, no. 2, pp. 494–498.
3. Danilov, M.O. and Melezhyk, A.V., *J. Power Sources*, 2006, vol. 163, no. 1, pp. 376–381.
4. Hsieh, C.-T., Lin, J.-Yi., and Wei, J.-L., *Int. J. Hydrogen Energy*, 2009, vol. 34, no. 2, pp. 685–693.
5. Wang, X., Waje, M., and Yan, Y., *Solid-State Lett.*, 2005, vol. 8, no. 1, pp. A42–A44.
6. Wang, G., Shen, X., Yao, J., and Park, J., *Carbon*, 2009, vol. 47, no. 8, pp. 2049–2053.
7. Xin, Y., Liu, J., Jie, X., et al., *Electrochim. Acta*, 2012, vol. 60, pp. 354–358.
8. Lin, Z., Waller, G., Liu, Y., et al., *Adv. Energy Mater.*, 2012, vol. 2, no. 7, pp. 884–888.
9. Qu, L.T., Liu, Y., Baek, J.B., and Dai, L.M., *ACS Nano*, 2010, vol. 4, no. 3, pp. 1321–1326.
10. Lin, Z.Y., Song, M.K., Ding, Y., et al., *Phys. Chem. Chem. Phys.*, 2012, vol. 14, no. 10, pp. 3381–3387.
11. Shao, Y., Zhang, S., Wang, C., et al., *J. Power Sources*, 2010, vol. 195, no. 15, pp. 4600–4605.
12. Kosynkin, D.V., Higginbotham, A.L., Sinitzskii, A., et al., *Nature*, 2009, vol. 458, pp. 872–876.
13. Danilov, M.O., Kolbasov, G.J., Rusetskii, I.A., and Slobodyanyuk, I.A., *Zh. Prikl. Khim.*, 2012, vol. 85, no. 10, pp. 1601–1605.
14. Hummers, W.S.Jr. and Offeman, R.E., *J. Am. Chem. Soc.*, 1958, vol. 80, no. 6, pp. 1339.
15. Park, S., An, J., Potts, J.R., et al., *Carbon*, 2011, vol. 49,

- no. 9, pp. 3019–3023.
16. Dubin, S., Gilje, S., Wang, K., et al., *ACS Nano*, 2010, vol. 4, no. 7, pp. 3845–3852.
17. Moon, I.K., Lee, J., Ruoff, R.S., and Lee, H., *Nat. Commun.*, 2010, 1:73. doi: 10.1038/ncomms1067.
18. Krishnamoorthy, K., Veerapandian, M., Mohan, R., and Kim, S.-J., *Appl. Phys. A*, 2012, vol. 106, no. 3, pp. 501–506.
19. Wang, G., Wang, B., Park, J., et al., *Carbon*, 2009, vol. 47, no. 1, pp. 68–72.
20. Sun, Z., Popa, D., Hasan, T., et al., *Nano Res.*, 2010, vol. 3, no. 9, pp. 653–660.
21. Eda, G., Lin, Y.-Y., Mattevi, C., et al., *Adv. Mater.*, 2009, vol. 21, no. 4, pp. 1–5.
22. Loh, K.P., Bao, Q., Eda, G., and Chhowalla, M., *Nat. Chem.*, 2010, vol. 2, doi: 10.1038/nchem.907.
23. Shang, J., Ma, L., Li, J., et al., *Sci. Reports.*, 2012, 2:792. doi: 10.1038/srep00792.
24. Hu, Y., Wang, K., Zhang, Q., et al., *Biomater.*, 2012, vol. 33, no. 4, pp. 1097–1106.
25. Li, D., Muller, M.B., Gilje, S., et al., *Nat. Nanotech.*, 2008, vol. 3, doi:10.1038/nnano.2007.451.
26. Galande, C., Mohite, A.D., Naumov, A.V., et al., *Sci. Reports*, 2011, 1:85. doi: 10.1038/srep00085.
27. Cuong, T.V., Pham, V.H., Tran, Q.T., et al., *Mater. Lett.*, 2010, vol. 64, no. 3, pp. 399–401.
28. Luo, Z., Lu, Y., Somers, L.A., and Johnson, A.T.C., *J. Am. Chem. Soc.*, 2009, vol. 131, no. 3, pp. 898–899.